Strongly enhanced free-exciton luminescence in microcrystalline CsPbCl3 films produced via the amorphous phase

Strongly enhanced free-exciton luminescence in microcrystalline $CsPbCl_3$ films produced via the amorphous phase

S. Kondo , T. Saito

Research Center for Development of Far-Infrared Region, Fukui University, Bunkyo, Fukui 910-8507, Japan

Abstract

High-quality $CsPbCl_3$ films composed of crystallites with narrow size distributions are achieved for various size levels, from microcrystalline to polycrystalline, by a novel heat-treatment method applied to the same amorphous films. Their photoluminescence is dominated by free-exciton emission at every size level without showing trapped-exciton emission in great contrast to the case for single crystals. The microcrystalline state shows more than an order of magnitude stronger free-exciton emission than the polycrystalline state, and exhibits intense stimulated emission under high-power excitation.

Keywords: B. $CsPbCl_3$; D. Luminescence; D. Exciton; D. Superradiance; D. Quantum confinement

1. Introduction

Many metal halides such as silver [1], thallium [2], copper [3], lead [4] or cadmium [5] halides, including their mixed systems [6], can be rendered amorphous by quench deposition yielding film samples. The amorphous films exhibit excellent transmittance below the absorption edge and have a well defined, characteristic crystallization temperature at which their absorption spectra drastically change in outline. The films, when crystallized at temperatures just above the crystallization temperature, are generally in a microcrystalline state, and change into polycrystalline state when they are subsequently annealed at higher temperatures. Many of the crystalline films produced via the amorphous phase, whether they are microcrystalline or polycrystalline in nature, show very high transmittance compared with (polycrystalline) films deposited onto hot substrates. These characteristics can be exploited for studying mesoscopic optical properties of microcrystals of metal halides (including their mixtures).

Many informative papers [7–22] have been reported on optical properties of $CsPbX_3$ microcrystals embedded in CsX or PbX_2 crystal matrices (X = Cl, Br). These studies are based on the measurement of photoluminescence of microcrystals thermally grown in Pb^{2+}-doped CsX crystals or Cs^{+}-doped PbX_2 crystals, and deal successfully with quantum size effects on excitons, such as confinement-induced blue shifts of exciton energy and confinement-induced changes in the decay kinetics of excitons, or aim at elucidation of growth kinetics of the microcrystals. However, concerning confinement-induced change in the luminescence intensity for exciton recombination, no study has been reported so far, presumably due to difficulty in the sample preparation. On the other hand, we have shown [23] that well identified, various crystalline (microcrystalline to polycrystalline) states can be achieved for $CsPbCl_3$ by suitable heat treatment of amorphous films of the compound. The microcrystalline state is characterized by a well-averaged microcrystallite size for which blue-shifted exciton resonance due to quantum size effect on the exciton is clearly observed even in the absorption spectrum. In the present work, various size levels of well-averaged microcrystallite sizes were achieved for the same starting amorphous films by a novel heat-treatment method. This

enabled us to directly compare exciton luminescence intensities among various size levels of the $CsPbCl_3$ microcrystals for the first time. To our knowledge, such a comparative investigation of confinement-induced changes (quantum size effect) in the exciton luminescence intensity has not been reported in any other compound so far for such extremely densely dispersed microcrystals (compared to those dispersed in bulk crystals) as those contained in the microcrystalline $CsPbCl_3$ films.

2. Experimental

We first prepared amorphous $CsPbCl_3$ films by quench deposition onto silica–glass substrates attached to a copper block cooled to 77 K, in order to prepare the high-quality microcrystalline (and polycrystalline) $CsPbCl_3$ films described above. The deposition was carried out in a vacuum of about 9×10^{-6} Pa using a tungsten basket heating element placed 8 cm in front of the substrate [4]. Then the films were subjected to rapid cycles of heating (up to above the crystallization temperature, 302 K [16]) and cooling (down to 77 K), in order to achieve various sizes of $CsPbCl_3$ crystalline products stepwise in the films. This was performed by means of shot-like IR laser irradiation of the films using a cw CO_2 laser (wavelength, 10.6 μm; power, 10 W), with the substrate kept in contact to the 77 K copper block. One shot caused one cycle of the rapid heating/cooling. The irradiation time per shot was in the range 10–3000 ms, depending on the desired crystalline sizes. For each run of the heating/cooling cycles, photoluminescence and absorption spectrum of the films were measured in situ on an liquid nitrogen-cooled CCD spectrometer equipped with a 0.47 m grating monochromator. A 500 W xenon lamp (in combination with a 0.5 m grating monochromator) and a 30 W deuterium lamp were used as the light sources for the photoluminescence and absorption measurements, respectively. The luminescence was recorded in the configuration of backward scattering normal to the film surfaces in order to minimize reabsorption, with the incident angle of the exciting light being 45°.

3. Results

First of all, we note that $CsPbCl_3$ has very different (by 1.0 eV) optical energy gaps between the amorphous (4.0 eV) and the crystalline (3.0 eV) states, with the latter being characterized by a very sharp Wannier-exciton resonance just above the gap [23]. Figs. 1 and 2 show the sequential changes in the absorption and photoluminescence spectra of $CsPbCl_3$ excitons, respectively, measured by the above-mentioned method with the resolution of the CCD spectrometer set at 0.2 nm (the measuring time per spectrum was 1 s and 20 ms for the luminescence and absorption

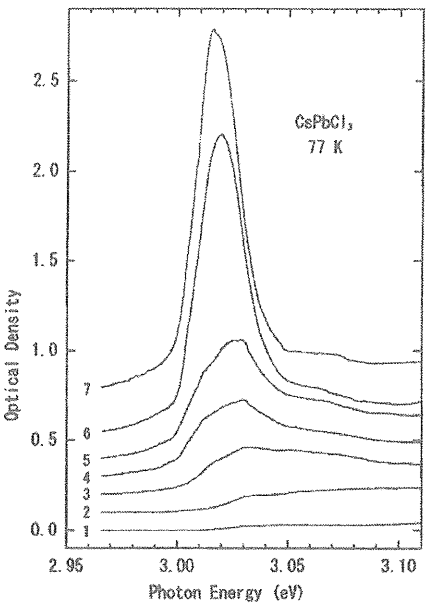

Fig. 1. The sequential change in the absorption spectrum of $CsPbCl_3$ excitons due to rapid heating/cooling cycles (see the text). The spectra are shifted along the Y axis for clarity.

spectra, respectively). The luminescence was excited at 3.3 eV, at which the starting amorphous $CsPbCl_3$ film exhibited excellent transmittance. The thickness of the film was 140 nm. The numbers, 1–7, in the figures indicate the orders of the runs of the heating/cooling cycles. The larger the numbers (run numbers), both the absorption and the luminescence spectra shifted to lower energies. On the other hand, although the absorption intensity monotonously increased with the run numbers, the luminescence was maximum in intensity for the third run (run number 3), after which the luminescence intensity decreased with increasing run numbers. Notably the absorption intensity was much weaker for the third run than for the last run (number 7); the last run was characterized by the biggest absorption peak and the weakest luminescence band. It was shown that the integrated (up to 4.0 eV) absorption intensity below 4.0 eV (where the $CsPbCl_3$ film was transparent in the amorphous state) remained almost unchanged after the third run, indicating completion of the film crystallization at the third run. The Stokes shift of the luminescence relative to the exciton absorption energy (which could be determined for the run number larger than 3) was very small: almost no Stokes shift was observed for the runs up to the fifth, and only about 3 and 11 meV of Stokes shift were recognized for the sixth and the last runs, respectively. The full width at half maximum (FWHM) of the luminescence band decreased with the run numbers from 28 meV (first run) to 18 meV (last run). We note that, although the luminescence measurements were made in the photon energy region down

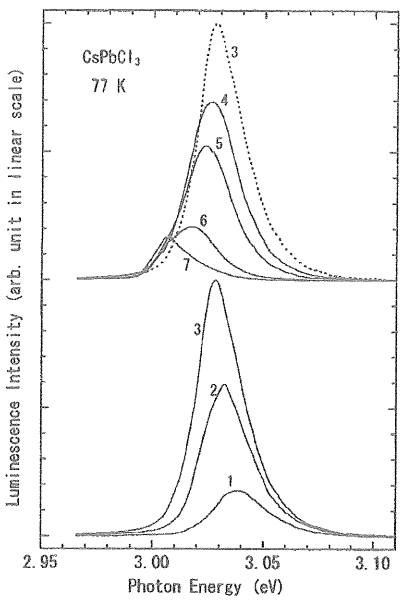

Fig. 2. The sequential change in the luminescence spectrum of $CsPbCl_3$ excitons due to rapid heating/cooling cycles (see the text), excited at 3.3 eV. The spectra are shifted along the Y axis, differently for curves 1–3 and 3–7, for clarity.

to 1.5 eV, no emission was observed below 3.1 eV for all the runs of the heating/cooling cycles.

The spectral red shift with increasing run numbers is attributable to relaxation of quantum confinement of the $CsPbCl_3$ exciton. The peak energy (3.016 eV) of the exciton absorption spectrum for the last run is very close to the exciton absorption energy (3.013 eV [23]) of polycrystalline $CsPbCl_3$ films. The resulting film (after the last run) is, therefore, considered to be nearly in the polycrystalline state. Conversely, the blue-shifted spectra occurring in the earlier stages of the heating/cooling cycles reflect the microcrystalline nature of the film (see Section 4). The blue shift of the luminescence spectrum for the first run, about 32 meV, corresponds to that of the quantum dots of a size of 4 nm embedded in CsCl crystals [8] (in Ref. [8], the sizes of the microcrystals are estimated from the blue shifts of the peak energies of the free-exciton emission bands relative to the smallest peak energy that is observed for suitably annealed samples, under the assumption of effective-mass approximation; the free-exciton radius is 1 nm). It is considered that fine microcrystallites of $CsPbCl_3$ were generated in the amorphous surroundings at the first and second runs and a microcrystalline film (with a filling factor of unity of the $CsPbCl_3$ microcrystal particles) was yielded in the subsequent runs. Thus the crystal growth from microcrystal to polycrystal occurred stepwise in the film during the first to the last heating/cooling cycles. We note that the luminescence for the polycrystalline state, though very weak in intensity compared to that for the microcrystalline state, was clearly observed at 340 K, in great contrast to the case for single crystals, where the luminescence is completely quenched at that temperature [24]. This suggests that even the polycrystalline film exhibits a higher luminescence efficiency than the single crystals.

To compare the luminescence intensities among different crystalline sizes (but the same equivalent thickness for the crystalline products) in the film, we normalized the luminescence spectra shown in Fig. 2 with respect to the absorbed intensity of the exciting light using the measured absorption intensity (at 3.3 eV). The result is shown in Fig. 3. It is seen that the microcrystalline films exhibit much stronger exciton luminescence than the polycrystalline film (for example, the integrated luminescence intensity for the second run was by more than an order of magnitude larger than that for the last run, see Section 4).

4. Discussion

Before discussing the results, it might be necessary to mention the method for investigating the change in the crystalline phase in the films, because the present experiment is based on in situ measurements of absorption and photoluminescence spectra of the films. For example, X-ray diffraction method is difficult to apply simultaneously to the in situ measurements. It is, however, well known that, as compared with X-ray diffraction method, exciton spectroscopy provides powerful means for investigating crystallinity of materials on a nanometer-scale when the materials

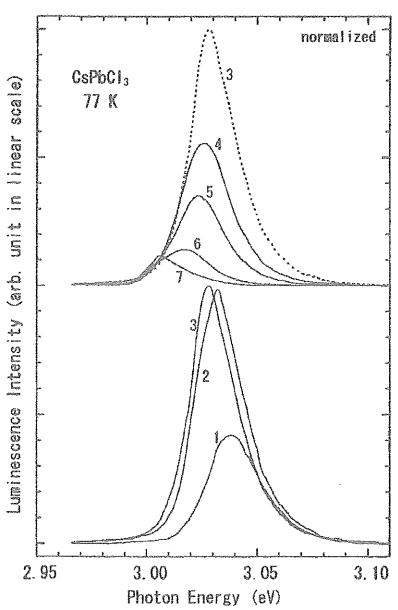

Fig. 3 The normalized luminescence spectra. The spectra in Fig. 2 are normalized with respect to the absorbed intensity of the exciting light.

show sharp exciton resonance [25]. In particular, spectral line-shape and peak energy and quantum yield for free-exciton luminescence are very sensitive to the state (or quality) such as lattice imperfections and size of microcrystals [26]. Therefore, free-exciton spectroscopy is frequently used for characterizing microcrystals or quantum dots [27]. In the discussion given below, we will use FWHMs and peak energies of the free-exciton emission bands to judge the quality, size and size-distribution of crystallites in the films (also, the absence of trapped-exciton emission is used as an indication for 'high-quality' of the crystallites).

The luminescence spectra presented in Section 3 are different in feature from any exciton luminescence spectra of $CsPbCl_3$ reported so far, i.e. bulk $CsPbCl_3$ crystals, $CsPbCl_3$ microcrystals in Pb^{2+}-doped CsCl crystals or Cs-doped $PbCl_2$ crystals and polycrystalline $CsPbCl_3$ films. For example, the luminescence spectrum of the bulk crystal measured at liquid nitrogen temperature [28] was composed of three bands, peaking at 2.987, 2.950, and 2.914 eV with the integrated intensity ratio of about 1:2:0.4 (which were deduced in Ref. [28] from the measured spectrum by a line-shape analysis using Gaussian fits). The highest-energy band was attributed to free excitons and the lower-energy bands to trapped excitons. At lower temperatures below 40 K, the free exciton luminescence became strongest in intensity. The FWHM of the free exciton luminescence band was almost the same (70–80 meV) in the temperature range at and below liquid nitrogen temperature. In polycrystalline films [29], a free exciton emission band (peak energy, 2.960 eV; FWHM, about 30 meV) was observed at 5 K together with weaker lower-energy emission due to trapped excitons. In Pb^{2+}-doped CsCl crystals or Cs^{+}-doped $PbCl_2$ crystals, complicated emission spectra were observed depending on the specimens heat-treated in different ways, and sometimes plate-like growth [7–9] of $CsPbCl_3$ micro-crystals occurred in a suitably heat-treated sample, exhibiting several emission bands due to recombination of free excitons confined in various $CsPbCl_3$ plates with different thicknesses. On the other hand, the present luminescence spectra were consistently composed of a single, free-exciton emission band with the larger peak energies (3.005–3.038 eV) and the smaller FWHMs (18–28 meV), without exhibiting any trace of trapped-exciton emission. The larger peak energies reflect quantum size effect on the free excitons confined within the microcrystallites (the larger peak energy 3.005 eV at 77 K than 2.960 eV at 5 K in Ref. [29], both for the polycrystalline state, is due to positive temperature coefficient [30] of the free-exciton energy) and the smaller FWHMs (i.e. smaller inhomogeneous line-broadenings) mean a high-quality nature and/or well-averaged size of the microcrystallites. The latter properties (high-quality nature and/or well-averaged size) of the microcrystallites should be stressed in view of the smaller FWHMs (at 77 K) than that at 5 K for the polycrystalline film. In particular, reflecting the high-quality nature of the microcrystallites, there is no trace of trapped-exciton emission. The absence of trap states for the free excitons means that lattice imperfections such as impurities and lattice distortions are drove away from the interior of the individual crystallites. It is notable that excitons even in the microcrystalline films are free from being trapped, despite the expectation [31] of a high density of surface states. To conclude, high-quality microcrystallites with narrow size-distributions are achieved at various size levels in the film by the fast heating/cooling operations carried out for the same starting amorphous film.

More noticeable feature exhibited by the present film is the strongly enhanced free-exciton luminescence in the microcrystalline state. For a quantitative comparison of the luminescence intensities between different crystalline states, we plotted, in Fig. 4, the integrated intensities of the normalized luminescence spectra (Fig. 3) versus the blue shifts in peak energies relative to the peak energy of the last spectrum (run number 7, polycrystalline state); all the data points are indicated by the run numbers. The X-axis of the plot can be viewed as a measure of the mean size of the crystallites in the film, that is, larger the X value, smaller the size (the data point 1 corresponds to the size about 4 nm as mentioned in Section 3). It is seen from the figure that the luminescence intensity for (the microcrystalline state with the mean size corresponding to) the blue shift of 26 meV amounts to about 11 times that for the polycrystalline state.

Baltog et al. [32] studied exciton luminescence under high-power excitation in single crystals of $CsPbCl_3$ and observed stimulated emission related to free-excitons for a particular optical configuration. Since the microcrystalline $CsPbCl_3$ films are characterized by the excellently strong free-exciton emission compared to that of single crystals as suggested above, they are expected to show much stronger stimulated emission than the single crystals. To demonstrate the expectation, we show in Fig. 5 an example of luminescence spectra (curves 1 and 2) of a very thin film

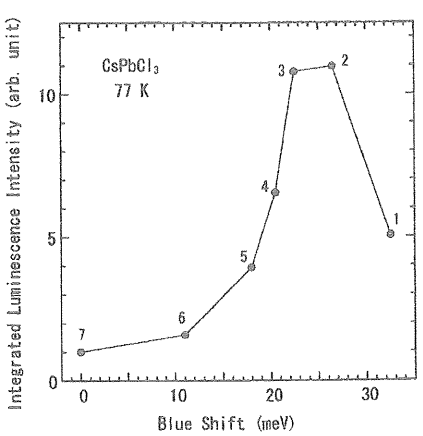

Fig. 4. The integrated luminescence intensity versus luminescence peak energy, plotted for the normalized luminescence spectra in Fig. 3 (see the text).

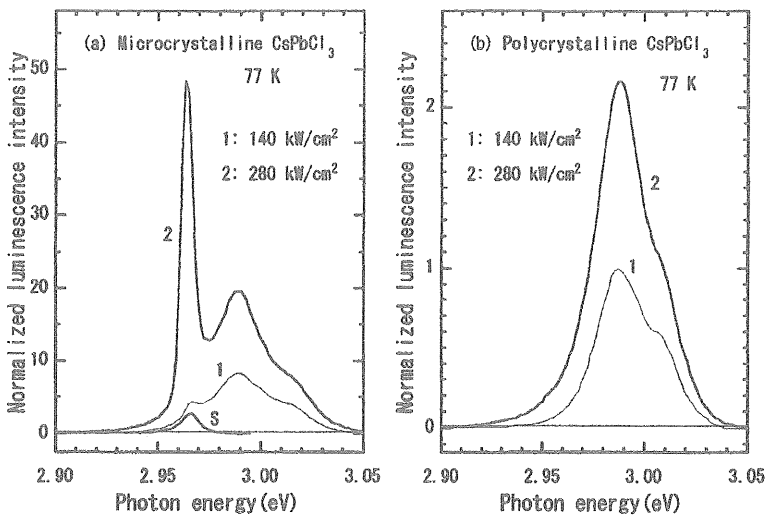

Fig. 5. The exciton luminescence spectra measured under high-power excitation for the microcrystalline (a) and polycrystalline (b) states of a film of 78 nm thickness.

(thickness, 78 nm), measured for the microcrystalline (a) and polycrystalline (b) states under high-power excitation using an N_2 laser (337 nm, 3.68 eV). The measuring optical configuration was the same (except the use of the N_2 laser instead of the xenon lamp and the monochromator) as that employed in the measurement of the spectra shown in Fig. 2. The crystallite-size levels for the microcrystalline and polycrystalline states correspond nearly to those for curves 5 and 7 shown in Fig. 2, respectively, as judged from the peak positions of the ordinary luminescence spectra (not shown in Fig. 5). The excitation power was 140 kW/cm^2 for curves 1 and 280 kW/cm^2 for curves 2. The spectra were so normalized that the peak value for curve 1 in (b) was unity. It is seen from the figure that the microcrystalline state exhibits about an order of magnitude stronger luminescence intensity than the polycrystalline state for equal excitation powers, roughly speaking. By spectral analysis curve 1 for the microcrystalline state could be decomposed into three bands, namely F (Lorentzian), X (Gaussian) and S (Lorentzian) bands in the order of decreasing photon energy; S band is plotted in the figure. Although F band, which corresponds to free-exciton recombination, and X band were yielded (by spectral analyses) from all the spectra in Fig. 5, S band, whose peak energy (2.965 eV) lies in the same photon energy range as that (2.963–2.968 eV) reported in Ref. [32] for stimulated emission, only showed up for the microcrystalline state. FWHM of S band was 10 meV for curve 1 and 8 meV for curve 2 (in (a)), which are very small compared to those (18–28 meV) for the free-exciton emission bands shown in Fig. 2. The ratio of the integrated intensities of S bands for curves 1 and 2 was 1:14, as compared to the ratio 1:2 of the corresponding excitation powers. We note that the excitation power under which the S-band integrated intensity amounted to 10 times that for curve 2 (in (a)) was 700 kW/cm^2 (2.5 times that for curve 2 in (a)). The rather exponential increase in the emission intensity with the excitation power, together with the spectral narrowing, for S band clearly indicates the occurrence of stimulated emission. We note that an onset of stimulated emission was also recognized for the polycrystalline state of the same film but under much higher-power excitation, above 2400 kW/cm^2 (17 times that for curve 1 in (a)).

The optical configuration employed by Baltog et al. for observing stimulated emission in single crystals is very different from the present one. They irradiated the crystals at 77 K with an N_2 laser and measured luminescence spectrum in a detection configuration in which the angle, ϕ, between the emitted light and the irradiated crystal surface was very small, about 9°. At excitation powers above 100 kW/cm^2, stimulated emission was observed, peaking at energies in the range 2.963–2.968 eV. However, it was difficult to observe stimulated emission for $\phi \sim 45°$. A long optical path within the irradiated crystals was required in order to evidence the occurrence of the stimulated emission, in great contrast to the case for the present microcrystalline films, where strong stimulated emission was easily observed for the very short photon path length (78 nm) in the film, as exemplified above. We note that thicker films showed intense stimulated emission compared to the case for single crystals, not only for the microcrystalline state but also for the polycrystalline state.

5. Conclusion

High-quality $CsPbCl_3$ films composed of crystallites with narrow size-distributions are achieved for various size

levels, from microcrystalline to polycrystalline, by a novel heat-treatment method of fast heating/cooling operations carried out for the same starting amorphous films. Reflecting the high-quality nature, the luminescence spectra of the films consistently exhibit a single, free-exciton emission band at every size level without showing trapped-exciton bands, unlike the case for single $CsPbCl_3$ crystals. The microcrystalline state shows more than an order of magnitude stronger free-exciton emission than the polycrystalline state. Very high (compared to the case for single crystals) quantum yields of the free-exciton emission can be expected for the microcrystalline state because even the polycrystalline state is characterized by more efficient free-exciton emission than the single crystals. In favor of the expectation, the microcrystalline state shows much stronger (rather, intense) stimulated emission than the polycrystalline state as well as than the single crystals, under high-power excitation. The extremely enhanced radiance in the microcrystalline films is of great interest in view of their application in opto-electronic microdevices; in particular, the intense stimulated emission is fascinating when considering application in thin-film lasers. Details concerning the stimulated emission will be reported elsewhere, including the results of lasing experiments as well as gain measurements.

Acknowledgements

The authors would like to acknowledge Professor H. Nakagawa for useful discussion.

References

[1] H.G. Gottwald, T. Lieser, K.G. Weil, A. Weiss, Z. Naturforsch. A 40 (1985) 677.
[2] S. Kondo, T. Itoh, S. Saito, M. Mekata, Solid State Commun. 78 (1991) 557.
[3] H.G. Gottwald, K.G. Weil, Ber. Bunsenges. Phys. Chem. 92 (1988) 60.
[4] S. Kondo, T. Sakai, H. Tanaka, T. Saito, Phys. Rev. B 58 (1998) 11401.
[5] S. Kondo, S. Kagawa, T. Saito, Phys. Status Solidi B 154 (1996) 583.
[6] S. Kondo, K. Amaya, T. Saito, Mater. Sci. Engng B 88 (2001) 85.
[7] R. Aceves, V. Babin, M. Barboza Flores, P. Fabeni, M. Nikl, K. Nitsch, G.P. Pazzi, R. Perez Salas, S. Zazubovich, Phys. Status Solidi B 225 (2001) 247.
[8] M. Nikl, K. Nitsch, K. Polak, E. Mihokova, S. Zazubovich, G.P. Pazzi, P. Fabeni, L. Salvini, R. Aceves, M. Barbosa-Flores, R. Perez Salas, M. Gurioli, A. Scacco, J. Lumin. 72–74 (1997) 377.
[9] M. Nikl, K. Nitsch, K. Polak, Phys. Rev. B 51 (1995) 5192.
[10] P. Fabeni, G.P. Pazzi, M. Nikl, K. Nitsch, A. Scacco, F. Somma, S. Zazubovich, S. Santucci, A.R. Phani, Electrochem. Soc. Proc. 97–29 (1998) 186.
[11] M. Nikl, K. Nitsch, E. Mihokova, K. Polak, G.P. Pazzi, M. Fabeni, F. Grioli, S. Somma, V. Zazubovich, A. Babin, S. Scacco, R. Santucci, R. Phani, M. Aceves, R. Barboza-Flores, Electrochem. Soc. Proc. 98–29 (1998) 250.
[12] K. Nitsch, V. Hamplová, M. Nikl, K. Polák, M. Rodová, Chem. Phys. Lett. 258 (1996) 518.
[13] M. Nikl, K. Nitsch, E. Mihokova, K. Polak, P. Fabeni, G.P. Pazzi, M. Gurioli, S. Santucci, R. Phani, A. Scacco, F. Somma, Physica E 4 (1999) 323.
[14] M. Nikl, K. Nitsch, E. Mihokova, K. Polak, P. Fabeni, G.P. Pazzi, M. Gurioli, R. Phani, S. Santucci, A. Scacco, F. Somma, Radiat. Eff. Defects Solids 150 (1999) 341.
[15] V. Babin, P. Fabeni, M. Nikl, G.P. Pazzi, I. Sildos, N. Zazubovich, S. Zazubovich, Chem. Phys. Lett. 314 (1999) 31.
[16] S.V. Myagkota, Opt. Spectrosc. 87 (1997) 311.
[17] S. Myagkota, A. Gloskovsky, A. Voloshinovskii, Opt. Spectrosc. 88 (2001) 538.
[18] A. Voloshinovskii, S. Myagkota, A. Gloskovskii, V. Gaba, J. Phys.: Condens. Matter 13 (2001) 8207.
[19] A. Voloshinovskii, S. Myagkota, A. Gloskovskii, S. Zazubovich, Phys. Status Solidi B 225 (2001) 257.
[20] A. Voloshinovskii, S. Myagkota, A. Gloskovskii, Phys. Solid State 43 (2001) 1885.
[21] R. Aceves, V. Babin, M. Barboza Flores, P. Fabeni, A. Maaroos, M. Nikl, K. Nitsch, G.P. Pazzi, R. Perez Salas, I. Sildos, N. Zazubovich, S. Zazubovich, J. Lumin. 93 (2001) 27.
[22] A. Voloshinovskii, S. Myagkota, A. Gloskovskii, S. Zazubovich, J. Lumin. 97 (2002) 198.
[23] S. Kondo, H. Mori, T. Saito, Phys. Status Solidi A 163 (1997) 445.
[24] L.N. Amitin, A.T. Anistratov, A.I. Kuznetsov, Sov. Phys. Solid State 21 (1979) 2041.
[25] M. Haselhoff, H.-J. Weber, Phys. Rev. 58 (1998) 5052.
[26] J.-S. Lee, in: Y. Masumoto, T. Takagahara (Eds.), Semiconductor Quantum Dots—Physics, Spectroscopy and Applications, Springer, Berlin, 2002, pp. 1–57.
[27] S.V. Gaponenko, Optical Properties of Semiconductor Nanocrystals, Cambridge University Press, Cambridge, 1998, pp. 84–152.
[28] M. Nikl, E. Mihokova, K. Nitsch, K. Polak, M. Rodova, M. Dusek, G.P. Pazzi, P. Fabeni, L. Salvini, M. Gurioli, Chem. Phys. Lett. 220 (1994) 14.
[29] F. Somma, P. Aloe, S. Lo, Mastro, J. Vac. Sci. Technol. B 19 (2001) 2237.
[30] I.P. Pashuk, N.S. Pidzirailo, M.G. Matsko, Sov. Phys. Solid State 23 (1981) 1263.
[31] F. Henneberger, J. Puls, in: F. Hennenberger, S. Schmitt-Rink, E. Göbel (Eds.), Optics of Semiconductor Nanostructures, Akademie, Berlin, 1993, pp. 497–543.
[32] I. Baltog, L. Mihut, S. Lefrant, J. Lumin. 68 (1996) 271.